Gait Modelling for a Context-Aware User-Adaptive Robotic Assistant Platform

Georgia G. Chalvatzaki, Xanthi S. Papageorgiou and Costas S. Tzafestas

***Abstract*—For a context-aware robotic assistant platform that follows patients with moderate mobility impairment and adapts its motion to the patient's needs, the development of an efficient leg tracker and the recognition of pathological gait are very important. In this work, we present the basic concept for the robot control architecture and analyse three essential parts of the Adaptive Context-Aware Robot Control scheme; the detection and tracking of the subject's legs, the gait modelling and classification and the computation of gait parameters for the impairment level assessment. We initially process raw laser data and estimate the legs' position and velocity with a Kalman Filter and then use this information as input for a Hidden Markov Model-based framework that detects specific gait patterns and classifies human gait into normal or pathological. We then compute gait parameters commonly used for medical diagnosis. The recognised gait patterns along with the gait parameters will be used for the impairment level assessment, which will activate certain control assistive actions regarding the pathological state of the patient.**

I. Introduction

The care of the constantly growing ageing population is a considerable problem for modern societies [1], [2]. One of the major issues we have to face is the mobility difficulties of the elderly, which can be caused either by age, or by certain pathologies. Walking problems affect not only the daily lives of the elderly but also their self-esteem, after they lose their ability to look after themselves. The lack of nursing staff, [3], in relation to the increased demands of the elderly for care, led scientists to turn to robotic assistants, since robotics can incorporate features such as posture support and stability, walking assistance, navigation in indoor and outdoor environments, health monitoring, etc.

Our motivation is to use intelligent robotic platforms (Fig.1), which can monitor and understand the patient's walking state and will autonomously reason on performing assistive actions regarding the patient's mobility and ambulation [4]. We are working on the development of an Adaptive Context-Aware Robot Control architecture, when the robotic assistant is in front of the user and detects the patient's mobility state by using real-time laser data. We recognise specific gait patterns and also compute gait parameters that are indicative of particular pathologies. The recognised parameters of the user are then used for the patient's mobility impairment assessment, and this indication will trigger certain control assistive actions and behaviours from the robotic assistant that follows the user. Such actions would be velocity adjustment of the platform, approach of the patient because of recognised changes in gait patterns due to fatigue, walking instability or due to the patient's will to perform another task (like approaching a chair to perform a stand-to-sit action).

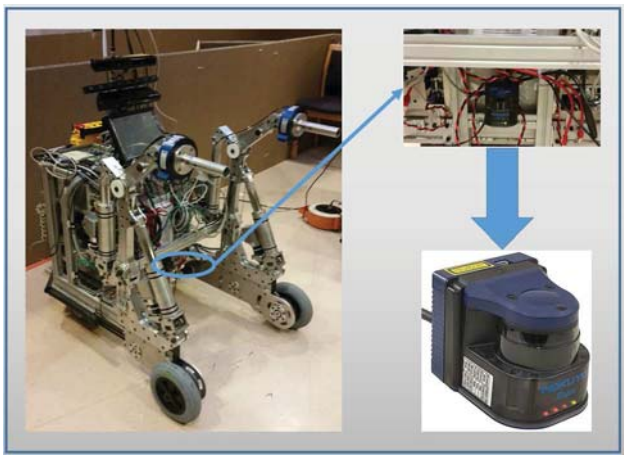

Fig. 1: A robotic platform equipped with a Hokuyo Laser Sensor aiming to record the gait cycle data of the user (below knee level).

In this paper we present our approach for the development of two procedures that are important for human gait modelling and their performance is necessary for the Adaptive Context-Aware Robot Control architecture. Firstly, we analyse the detection and tracking of the patient's legs, based on a Kalman Filter (**KF**), for estimating the legs' kinematic parameters. This process has the potential to track the user while performing straight walking, but also can overcome leg occlusions and false detections. Also, this is an essential part of the preprocessing of the raw laser data and it actually provides the input signal for our control architecture. Secondly we describe the development of a non-invasive framework for pathological walking recognition, based on a Hidden Markov Model (**HMM**), used for gait modelling and classification. This framework is designed to actively incorporate many different gait patterns as a subsystem within a larger cognitive behaviour-based context-aware robot control framework (that embodies several walking morphologies, including turning and maneuvering motions). Furthermore, this framework has the potential to be used for the classification of various walking pathologies and related impairments, and for actively and cognitively being augmented with new patients with mobility

This research work was supported by the European Union under the project "MOBOT" with grant FP7-ICT-2011-9 2.1 - 600796.

The authors are with the School of Electrical and Computer Engineering, National Technical University of Athens, Greece, gchal@central.ntua.gr, xpapag@mail.ntua.gr, ktzaf@cs.ntua.gr

In Proc. of the 8th International Conference on Integrated Modeling and Analysis in Applied Control and Automation (IMAACA), September, 21-23 2015, Bergeggi, Italy

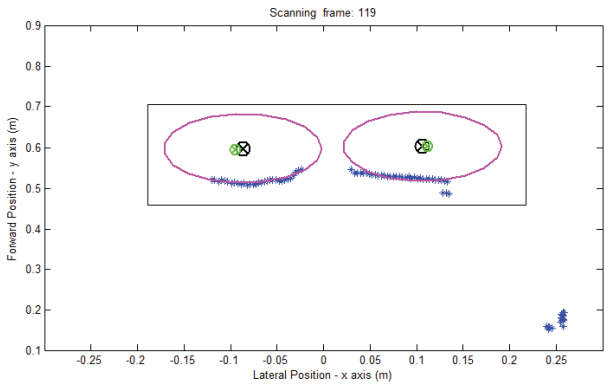

Fig. 2: Snapshot of the detected leg's from range data in the saggital plane. Blue stars correspond to the raw laser data; black 'X' correspond to the detected leg centers; green 'X' correspond to the estimated positions. The rectangle is the search window.

difficulties.

II. Related Work

As mobile robots are becoming more and more autonomous, the robot-following-human concept is getting popular in assistive robotics, and they are actually using various sensing technologies for monitoring human activity [5], [6]. The automatic classification and modeling of specific physical activities of human beings is very useful for the development of smart walking support devices, aiming to assist motor-impaired persons and elderly in standing, walking and other mobility activities, as well as to detect abnormalities and to assess rehabilitation procedures [7]–[11]. For the extraction of gait motions, different types of sensors have been used, from gyroscopes and accelometers to cameras, etc., [12]–[16]. Other approaches refer to human detection and tracking, or recognition of human activity utilizing laser sensors, and in some cases complementary with cameras, or force sensors, [17].

For the robot-following-human problem, there is a discrimination in positioning between human and mobile robot; robot following human from behind, or by the side of the human, or in front of the human. Towards this direction, the estimation of the legs' kinematic parameters with respect to the mobility aid is essential. Thus, the detection and tracking of humans is a common problem. Most research work focuses on detecting and tracking human legs from static sensors, as in pedestrian tracking, [18], or from laser scanners mounted on mobile robotic platforms for person following [19], where several tracking and control methods have been applied, [20], [21]. The need for a substantial interaction between human and accompanying robotic platform led to the development of sophisticated control schemes for a high level understanding of the human behavior, presenting early research results in [22]–[25]. Most gait tracking methods use standard Kalman Filters, for which normal gait is modeled as an interchange of accelerative and decelerative motions of the two legs [26], with predefined filter inputs for the motion models. However, those models are had to be applied to pathological gait. Mobility impairment of different origin result in different gait patterns. In this work, we present a gait detection and tracking method that is easy to implement, that uses a standard Kalman filter, using acceleration as the system's noise, and also uses the predicted state vector as feedback of the tracking process for the detection of the user's legs for the next time frame.

A key issue for the development of a context-aware robotic assistant platform that monitors elderly people with mobility inabilities, is gait modelling, i.e. the extraction of specific gait patterns that correspond to specific pathologies, and will be necessary for the assessment of the mobility impairment level of the subject, that will trigger certain assistive actions from the robotic assistant. The dynamic properties of walking led to the usage of Hidden Markov Models **(HMMs)**. Time series data can be modelled by HMMs, since they are not only easy to build and manipulate, but also to train and score them with optimal algorithms (e.g. maximum likelihood, Viterbi decoding). In HMMs only the output of the model is visible to the observer and the states of the model (corresponding to a physical event) are not observable, in other words are hidden, [27]. The versatility of HMMs makes them useful in extracting human patterns. Apart from their prominent application in speech recognition, [28], HMMs are also used in a number of pattern recognition applications, gesture recognition, [29], human activity analysis, [30] and biometric gait recognition, [31]. The first attempts to model the normal walking motion by using HMMs with respect to laser data features, were presented in [32], [33]. In this work we extend this approach to model and characterize the pathological walking motion, in order to integrate it into a Context-Aware Robot Control.

III. System Overview

An Adaptive Context-Aware Robot Control architecture is being developed for the intelligent robotic assistant platform, that will adapt and act according to the patient's needs. The system is driven by the sensory data of a 2D laser range scanner that detects the walking motion (Fig.1). An important step for performing behavior-based context aware control is the preprocessing of the system's input signal. This process incorporates the detection and tracking of the user's legs. This framework takes as input the noisy laser data, detects the patient's legs and estimates their actual position and velocity with respect to the robotic assistant. The estimated kinematic state of the subject's legs feed the cognitive context-aware control system as the environmental input signal, that is used to infer the context (i.e. state of the patient) and to perform specific actions in the detected context.

The control scheme consists of the typical three-layer architecture. The high level of this control scheme contains the Gait Modelling and Classification module. This is an HMM-based approach that can recognize sequences of gait patterns

and also it can classify them into normal pathological ones, or non-walking activity. Given the spatiotemporal properties of those sequences, we compute particular gait parameters (such as step length, cadence), that are commonly used for medical diagnosis, [34], since differentiations in their values are indicative of specific pathological states. In that way, an impairment level assessment is performed, for completely knowing the context of the patient's walking motion (i.e. recognition of the patient's intention to walk, gait modelling, estimation of the subject's pathological status).

This context-awareness is used as input to the medium level control module. Medium level control contains specific behaviours and assistive actions, that are activated according to the subject's detected context. The robotic assistant should adaptively track and follow the subject during its walking motion. Also the platform should smoothly stop in front of the subject in cases when the subject freezes and stops abruptly. Furthermore, the platform should smoothly approach the user to provide possible support when instability in gaiting is detected.

All this information is used as input to the typical low level controller of the platform, in order to inherently translate the decision of performing a specific assistive action into motor commands.

IV. Preprocessing of Control Input: Leg Detection and Tracking

For the detection and tracking of the patient's legs we use a combination of K-means clustering to detect the subject's legs and a Kalman Filter for tracking the user, and therefore estimate of the kinematic parameters of walking, i.e. the legs' positions and velocities. Our approach is a recursive system with a substantial forward-backward interaction between the detection and tracking of the user.

A. Data Processing and extraction of candidate legs

The raw laser data are processed at each time frame. Data processing consists of defining an observation window (a rectangle area) in the scanning plane of the laser scanner. The window's initial dimension is computed by the area in front of the rollator, where we expect the subject to be standing before performing the walking task. This initial search window is predetermined and wide enough, while in the subsequent frames it is adjusted. For the data inside the window we use a simple background extraction method based on thresholding criteria. The laser points that lie outside the observation window are discarded, while the remaining are separated into groups, corresponding to detected objects according to the Euclidean distance between consecutive laser points. In cases of discontinuities of laser points, due to fluctuations of the device, or due to the objects deformable surface (common in creasing pants), instead of having one laser group describing an object, we end up with more. In such cases the adjacent laser groups are merged according to an euclidian threshold. Finally, any laser group that contains less than a specific number of points is deleted. The remaining laser groups formulate the candidate legs. The candidate legs extraction is successful when we end up with two candidates, corresponding to the legs. The treatment in cases of less or more laser groups is described bellow.

B. Legs' Detection

The candidate legs feed the Legs' Detection subsystem, by using a K-means++ clustering algorithm [35], that classifies the left and right leg. Instead of using the highly noisy centroid-mean of each cluster given by K-means, we take as consensus that the human limbs can be represented as cylinders, and therefore can be seen as circles in the scanning plane. We use nonlinear least squares circle fitting with a constant pre-computed radius, in order to approach the actual planar leg centers. In that way we have a compact representation of the legs, which is not influenced so much by the shape deformations of the laser groups. The detected legs' centers compose the observation vector z_k for the tracking process.

C. Kalman Filter Tracking

The tracking of the user's legs is performed by a discrete Kalman filter **(KF)** algorithm [36], using as observation vector z_k the detected leg centers at each time frame. For the description of the legs' motion we used a second order kinematic model, i.e. it incorporates the position and velocity of the legs, and subsequently the used state vector has eight parameters:

$$x_k = [\ x^L \quad y^L \quad x^R \quad y^R \quad v_x^L \quad v_y^L \quad v_x^R \quad v_y^R\ ] \tag{1}$$

where (x^L, y^L) ,(x^R, y^R) are the positions and (v_x^L, v_y^L), (v_x^R, v_y^R) the velocities of the left and right leg along the axes. The Kalman Filter process equation has the form:

$$x_{k+1} = A_k \cdot x_k + B_k \cdot w_k \tag{2}$$

where A_k is the transition matrix and it has the following form:

$$A_k = \begin{bmatrix} I_4 & A_1 \\ \emptyset_4 & I_4 \end{bmatrix} \tag{3}$$

where $A_1 = \Delta t \cdot I_4$, and I_4 is the 4x4 identity matrix. The gain matrix B_k is multiplied with the process noise w_k and is given by:

$$B_k = \begin{bmatrix} B_1 \\ B_2 \end{bmatrix} \tag{4}$$

where $B_1 = (\Delta t^2/2) \cdot I_4$, $B_2 = \Delta t \cdot I_4$, I_4 is the 4x4 identity matrix. The uncorrelated process noise w_k is white and gaussian, and is given by the distribution $w_k \sim N(0, Q_k)$, where Q_k is the process noise covariance matrix. Since we have no known control inputs, we assume that acceleration is the effect of an unknown input and we treat the acceleration as the process noise. Therefore, it represents the influence of acceleration's variability at the state parameters at each time instant k. The process noise covariance matrix Q_k, which is an 8x8 square matrix, is computed by:

$$Q_k = B_k \cdot C_a \cdot B_k^T \tag{5}$$

where C_a is the covariance matrix of the acceleration a, with $a \sim N(0,C_a)$ and C_a is a 4x4 diagonal matrix with diagonal elements: $std^2_{La_x}, std^2_{La_y}, std^2_{Ra_x}, std^2_{Ra_y}$ where $std_{La_x}, std_{La_y}, std_{Ra_x}, std_{Ra_y}$ are the standard deviations of the accelerations along the axes for both legs, that were experimentally defined and describe the acceleration uncertainty throughout the gait.

The observation vector z_k of the true state is updated according to the equation:

$$z_k = H_k \cdot x_k + v_k \tag{6}$$

where H_k is the observation matrix which maps the true state space into the observed space:

$$H_k = \begin{bmatrix} I_4 & \emptyset_4 \end{bmatrix} \tag{7}$$

with $\emptyset_4$ is the 4x4 zero matrix, and v_k is the observation noise, with normal probability distribution $p(v_k) \sim N(0,R_k)$, where R_k is the measurement noise covariance matrix, a 4x4 diagonal matrix with the following form:

$$R_k = \begin{bmatrix} {v_{x_k}}^2 & 0 & 0 & 0 \\ 0 & {v_{y_k}}^2 & 0 & 0 \\ 0 & 0 & {v_{x_k}}^2 & 0 \\ 0 & 0 & 0 & {v_{y_k}}^2 \end{bmatrix} \tag{8}$$

where v_{x_k} and v_{y_k} for both legs are the standard deviations of the measurement noise v_k along the axes. KF is a recursive Bayesian estimator that consists of two phases,(i) the prediction and (ii) the update phase. During prediction phase the KF projects the state vector and the state covariance matrix forward in time according to the physical model of the process described by the input matrix A_k, and provides the *a priori* state estimate:

$$\widehat{x}_{k|k-1} = A_k \cdot \widehat{x}_{k-1|k-1} \tag{9}$$

and the *a priori* estimate covariance:

$$P_{k|k-1} = A_k \cdot P_{k-1|k-1} \cdot {A_k}^T + Q_k \tag{10}$$

In the update phase, the observation vector serves as a feedback that corrects the a priori estimates. Thus, the observation innovation is computed by:

$$\widetilde{y}_k = z_k - H_k \cdot \widehat{x}_{k|k-1} \tag{11}$$

and its innovation covariance:

$$S_k = H_k \cdot P_{k|k-1} \cdot {H_k}^T + R_k \tag{12}$$

Innovation is crucial for obtaining the Kalman gain. The Kalman gain is the solution to the minimum mean square error in the posterior state estimation, and is given by:

$$K_k = P_{k|k-1} \cdot {H_k}^T \cdot {S_k}^{-1} \tag{13}$$

Kalman gain technically calculates the quota of the predicted state estimate and the measurement into the final *a posteriori* state estimation. In that way we get the *a posteriori* state estimate:

$$\widehat{x}_{k|k} = \widehat{x}_{k|k-1} + K_k \cdot \widetilde{y}_k \tag{14}$$

and the *a posteriori* estimate covariance:

$$P_{k|k} = (I - K_k \cdot H_k) \cdot P_{k|k-1} \tag{15}$$

At each time instant, the detection process provides the observations for the KF tracking, and the KF feeds the system back with the predicted state vector $\widehat{x}_{k|k-1}$. Especially the legs' predicted positions are used as seed for the K-means++ algorithm, as an inference to where it should assign the leg clusters in the next frame. Around the predicted positions of the legs, leg-windows are set having initial constant dimensions proportional to the leg-circle's dimensions. The leg-windows dimensions are also adaptively adjusted, by enlarging or shortening them according to the variability of the predicted positions, provided by the *a priori* estimate covariance $P_{k|k-1}$ derived by the KF. From the two leg-windows, a wider search window is defined in the plane and the detected raw data inside it are ready to be processed. Thus, the described process results in an iterative interaction between detection and tracking processes. Finally, the estimated state vector $\widehat{x}_{k|k}$ enters the HMM Gait Phases Recognition System as an observation at each time frame.

D. False Detection Treatment

False detections are the cases in which either one leg is occluded by the other or there is interference of another person's legs inside the search window that have not been successfully discarded. Those cases can interrupt or contaminate the detection and can result in losing track of the legs. To address such false detections, certain hypotheses are checked. If the detected leg centers violate a Euclidean distance constraint that we have set, relevant to an experimentally defined anatomical threshold, or when there are detected less or more than two laser groups, the corresponding detection is regarded false. In order to continue to the tracking phase, an only-prediction Kalman filter is applied. In that particular case, we perform only the prediction step and we use the prediction state vector $\widehat{x}_{k|k-1}$ and the *a priori* estimate covariance $P_{k|k-1}$ as feedback for the detection of the next frame, without taking into consideration any observations for that particular time frame. This choice has been made, as it was noticed that between two consecutive frames the leg positions are not so prone to sharp or sudden shifts.

V. HMM Gait Modelling

Hidden Markov Models are well suitable for gait recognition because of their statistical properties and their ability to reflect the temporal state-transition nature of gait. An HMM is defined as a doubly embedded stochastic process with an underlying process that is not observable (it is hidden), but can only be observed through another set of stochastic processes that produce the sequence of observations, [27]. This reveals that the states underlying the data generation process are hidden, and they could be inferred through observations.

This HMM based model is performed in the high level of the Adaptive Context-Aware Robot Control, which utilizes as observables several quantities that represent the motion of

the subjects' legs (relative position w.r.t. the laser, velocities, etc.), which are estimated sequentially by the detection and tracking module, while the robotic assistant platform follows the subject's motion.

In this paper we have used the gait phases that characterize the gait cycle. The gait cycle describes the period of time during which one leg leaves the ground for the first time to perform a forward motion till when the same leg contacts the ground again, [37]. Each gait cycle has two phases: stance and swing. In stance the foot is in contact with the ground. In swing the foot is in the air performing a ballistic motion. The gait cycle is divided into eight events:

1) *IC* - Initial Contact: 0% of gc[1]
   Heel strike initiates the gait cycle and represents the point at which the body's centre of gravity is at its lowest position.
2) *LR* - Loading Response: 0-10% of gc
   Foot-flat is the time when the plantar surface of the foot touches the ground.
3) *MS* - Midstance: 10-30% of gc
   Midstance occurs when the swinging (contralateral) foot passes the stance foot and the body's centre of gravity is at its highest position.
4) *TS* - Terminal Stance: 30-50% of gc
   Heel-off occurs as the heel loses contact with the ground and pushoff is initiated via the triceps surae muscles, which plantar flex the ankle.
5) *PW* - Preswing: 50-60% of gc
   Toe-off terminates the stance phase as the foot leaves the ground.
6) *IW* - Initial Swing: 60-70% of gc
   Acceleration begins as soon as the foot leaves the ground and the subject activates the hip flexor muscles to accelerate the leg forward.
7) *MW* - Midswing: 70-85% of gc
   Midswing occurs when the foot passes directly beneath the body, coincidental with midstance for the other foot.
8) *TW* - Terminal Swing: 85-100% of gc
   Deceleration describes the action of the muscles as they slow the leg and stabilize the foot in preparation for the next heel strike.

Since the TW phase is characterized by heel strike that is an equivalent trigger to the IC phase, and therefore those phases are treated as identical. These seven states can define the hidden states of the HMM (Fig. 3). The state and observations at time t are denoted as s_t and O_t, respectively. The seven states at time $t = 1,2,...,T$, where T is the total time, are expressed by the value of the (hidden) variable $s_t = i \in \mathbf{S}$, for $i = 1,\ldots,7$, where $1 \equiv IC/TW$ (since we treat IC and TW as identical), $2 \equiv LR$, $3 \equiv MS$, $4 \equiv TS$, $5 \equiv PW$, $6 \equiv IW$, and $7 \equiv MW$. Regarding observations at time t, we define nine signals denoted as x^m, y^m, υ_x^m, υ_y^m, for $m = \{R,L\}$, which are the coordinates and the velocities along the axis for right and left leg, respectively, and *Dlegs* which is the distance between legs, that are represented by the vector $O_t = [o_t^1 \ldots o_t^k]^T \in \mathbf{O}$, for $k = 1,\ldots,9$, where $o_t^1 \equiv x^R$, $o_t^2 \equiv y^R$, $o_t^3 \equiv x^L$, $o_t^4 \equiv y^L$, $o_t^5 \equiv \upsilon_x^R$, $o_t^6 \equiv \upsilon_y^R$, $o_t^7 \equiv \upsilon_x^L$, $o_t^8 \equiv \upsilon_y^L$, and $o_t^9 \equiv Dlegs$. The observation data (derived from the raw laser sensor data) are modeled using a mixture of Gaussian distributions. This is a natural way of representing these data, as the data vector takes values from a bounded set (recall that we use the relative position of the legs from a robot that follows the subject with his/her mean velocity) and is inherently repetitive (due to the cyclic nature of the human gait). Thus, by collecting many data for a normal gait, we can obtain the mean and the variance of the Gaussian distributions of the mixture. Since nine signals are measured and constitute the extracted features at each time instant, the distribution is a multivariate Gaussian distribution:

$$g(x|\mu_m,\Sigma_m) = \frac{1}{(2\pi)^{\frac{n}{2}}|\Sigma_m|^{\frac{1}{2}}} \exp\left\{-\frac{1}{2}(x-\mu_m)^T\Sigma_m^{-1}(x-\mu_m)\right\}$$

where $x \in \mathbb{R}^n$ is the feature vector, $\mu_m \in \mathbb{R}^n$ denotes the mean vector and Σ_m denotes the $(n \times n)$ covariance matrix of the m^{th} Gaussian probability density, where in our case $n = 9$, and $m = 1,\ldots,M$. The Gaussian Mixture Model (GMM) is then a weighted sum of these M component Gaussian densities, as given by the equation:

$$P(x) = \sum_{m=1}^{M} w_m \cdot g(x|\mu_m,\Sigma_m)$$

where w_m are the mixture weights, for which it holds:

$$\sum_{m=1}^{M} w_m = 1,\ w_m \geq 0.$$

In normal gait cycle the gait phases follow each other sequentially, while in pathological gait the sequence of gait phases may be different or some of them may disappear. Thus, this HMM is a left-to-right model.

VI. Gait Parameters Computation for Medical Diagnosis

The analysis of gait patterns for medical diagnosis is presented in [34], by using different types of wearable and non-wearable sensors and by extracting and employing various gait parameters, [38].

The recognized sequence of gait phases is indicative of the subject's underlying pathology, since it differs from the normal gait phase sequences. We can, also, take advantage of the segmentation in time that the recognition system provides, regarding the duration of each gait phase, in order to compute specific gait parameters from the range data, that are necessary to specialists to perform medical diagnosis of the subject, [38]. The recognised gait patterns along with the gait parameters will be used by the robotic platform for the assessment of the patient's impairment level, which will trigger specific behaviours and assistive actions by the robotic assistant platform, in the medium level of the Adaptive Context-Aware Robot Control. For the impairment level assessment, we are computing the following gait parameters, [38]:

[1]gc: abbreviation for gait cycle

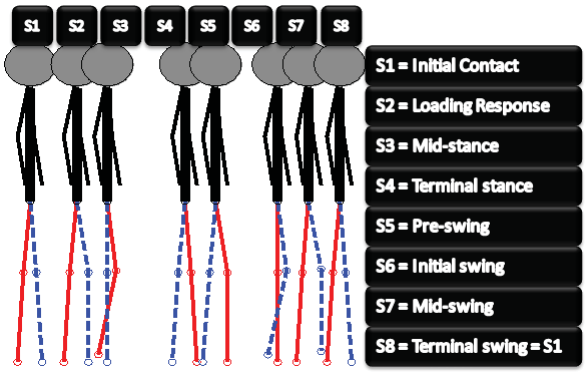

Fig. 3: Internal states of normal gait cycle (Left Leg: blue dashed line, Right Leg: red solid line).

1) Step length (linear distance between two successive positions of the same leg)
2) Stride length (linear distance between the positions of both feet)
3) Cadence (number of steps per time unit)
4) Step width (lateral distance between the two legs)
5) Stance time (time from IC to TS)
6) Swing time (time from IW to TW).

VII. Experimental Results

A. Experiment Description and Dataset

The experimental data used in this work were collected in Agaplesion Bethanien Hospital/ Geriatric Center with patients that presented moderate to mild impairment according to clinical evaluation of the medical associates. We have used a Hokuyo rapid laser sensor (UBG-04LX-F01 with mean sampling period of about 28msec) mounted on the robotic platform.

For the evaluation of our algorithmic approach, we have used the recorded data of seven patients with moderate mobility impairment (aged over 65 years old), performing a scenario during which the subject walked unassisted, i.e. without any physical support of the carer or the robotic platform, the subject walked straight in a walkway, while the robotic platform moved in a near distance in front of the subject (following mode).

B. Detection and Tracking results

For the experimental evaluation of the Detection and Tracking system, we had experimentally defined the thresholds used in the preprocessing of the laser data. A crucial feature for the performance of the KF tracking is the fine tuning of the filter to achieve its convergence to the true state. Since we did not have any ground truth data, KF tuning was difficult to achieve. As far as it concerns the measurement noise, given that only three points are sufficient to define a circle, we conducted Markov Chain Monte Carlo sampling for the three point in the circle's contour, using the information about the nominal noise of the laser scanner (considered to be white and gaussian with standard deviation $\sigma_{laser} = 0.0025m$. With those random samplings we have simulated how the random disturbances of the three points on the circle's contour introduced by the laser's error can deviate the estimated circle center through nonlinear circle fitting (given a known radius). On the other hand, the process noise statistics were trained by raw data.

However, the described experimentation led to an overestimation of the process noise parameters and an underestimation of the measurement noise statistics that resulted in overfitting problems. This seems quite reasonable, since human leg's locomotion cannot be accurately described by a linear motion model, and also measurement noise influenced by other parameters that cannot be simulated, e.g. the laser clusters deformable shapes due to the patient's clothing. In order to achieve the filter's convergence, we have followed the presented methodology of [39]. The resulted noise parameters are as follows:

- For the computation of the process noise covariance matrix in (5), we need the acceleration's covariance matrix, where: $std_{La_x} = 4.62$, $std_{La_y} = 9.1$, $std_{Ra_x} = 2.63$, $std_{Ra_y} = 8.38$ (in m/sec^2).
- For the measurement noise covariance matrix in (8), we resulted to the following standard deviations: $v_{x_k} = 0.05$ and $v_{y_k} = 0.01$ (in m).

In Fig. 2 a snapshot of the detected user's legs from laser range data is presented. The raw laser data are represented by blue stars, the detected leg centers with black x's and their estimated positions with green x's. Each subfigure depicts the rectangle observation window that isolates the raw laser data (blue stars) that are likely to correspond to legs. The raw laser data incorporate both the user's legs and outliers. On the detected leg clusters, fitted circles are drawn and the circles' centers (black x's) are the observations used in the KF tracking phase that estimate the leg's positions (green x's).

In Fig. 4 and Fig. 5 the detected (magenta and green stars) and the estimated (solid blue and red lines) for the lateral and forward displacement of the left and right leg accordingly, are shown. Also, in Fig. 6 the estimated and computed velocities are depicted (computed by differentiating over time the detected legs' positions). For the evaluation of the KF performance, we have computed the root mean square errors **(RMSE)** between the estimated and detected positions of the legs. In the absence of ground truth data, we regard the computed RMSE a measure of how much the KF improves the noisy observations. The average RMSE computed over the results of the detection and tracking process of the 7 patients that performed the same task, were 0.0078m for the x coordinate (lateral motion) and 0.0018m for the y coordinate (forward motion). In the lateral plane there is greater uncertainty (about 4 times bigger), due to the leg clusters shape deformability and length variability. In the absence of ground truth data, we are not able to accurately evaluate the results of the computed RMSE. However, we observed that the deformability of the leg clusters caused greater variability in the lateral plane, which is generally not wanted (gaiting is mainly taking place in the forward direction towards the rollator, thus sudden lateral

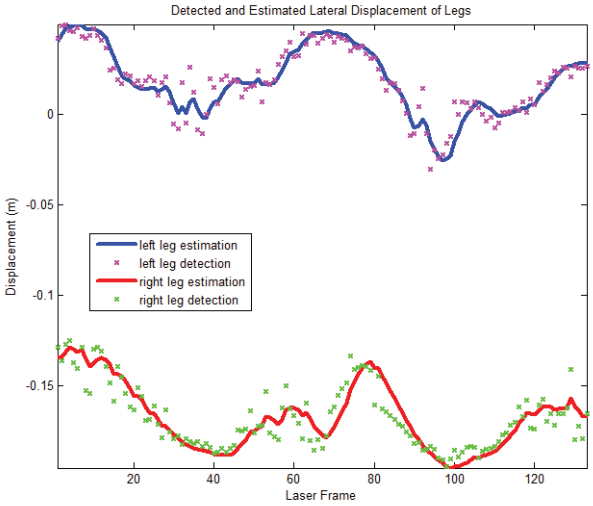

Fig. 4: Detected and estimated legs' lateral displacement.

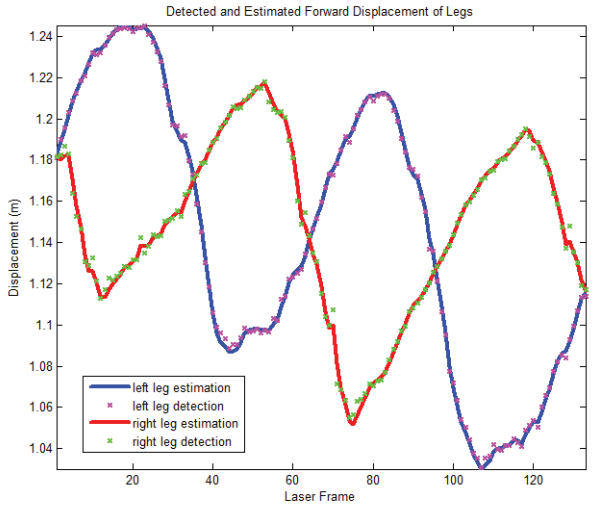

Fig. 5: Detected and estimated legs' forward displacement.

motions are artifacts), we can say that our method smooths out the noise in the lateral motion, rather than in forward motion, where we desire a smoother but closer tracking of the observations in that direction. In order to evaluate the results of our tracking method, we are currently working on extracting motion capture data to use as ground truth.

C. Gait Phases Recognition Results

HMM training procedure comprises only a part of subjects' data, excluding the recorded data of one subject. The testing procedure aims to test the performance of the proposed approach, validating its generalisation capacity over unseen data obtained by new subjects. The evaluation is based on an assessment of the estimated states provided by the constructed HMM, which represents the human gait cycle.

For testing and evaluation purposes of the constructed

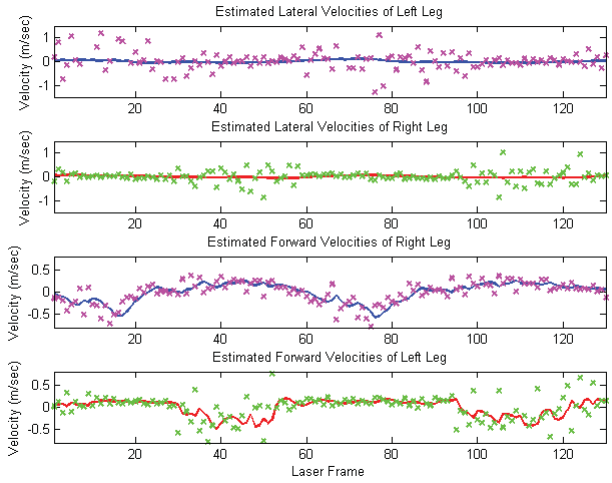

Fig. 6: Detected and estimated legs' velocities along the axes.

HMM, we have demonstrated an example of the real experimental data set which is depicted in Fig. 7. The goal of this evaluation phase is to unveil the hidden parts of the constructed models, i.e. to estimate the correct sequence of phase transitions that occur in the test data. This test dataset reflects the gait session of one elderly subject, and comprises about seven walking sections (about seven strides[2]). In this figure the displacement of each leg in the sagittal plane with respect to time is depicted on the top graph, while the bottom graph shows the evolution of the distance between legs within the same time frame. This figure is very useful to understand the exact subject's motion. The walking session is starting with the left leg, and it is obvious from the increasing of the distance between the legs that the early gait phases are occurred, Fig. 7. While this distance is going to zero (crossing point) the right leg is moving forward until the next crossing point. It can be observed that the first complete stride is recognized to begin just after the 6*sec*. This is observable to the results of the constructed HMM in Fig. 8, since at the time instant just after the 6*sec*, a gait cycle is started by the recognized IC phase.

The estimated sequence of gait phases obtained using the trained model is depicted in Fig. 8. This figure shows the time instant at which each gait phase (hidden state of HMM) is activated. A first remark that can be made by observing these experimental results is that the evolution of the gait phases provided by the models matches the general evolution of the human gait model that is to be represented by the HMMs; i.e. the gait phases appear sequentially with the correct order, and the time frame of each phase is within the general bounds as have been mentioned previously in Section V. It is obvious that some of the gait phases are omitted, since these experimental data corresponds to a subject with walking difficulties related

[2]Stride is the equivalent of gait cycle, i.e. two sequential steps define one stride, [40].

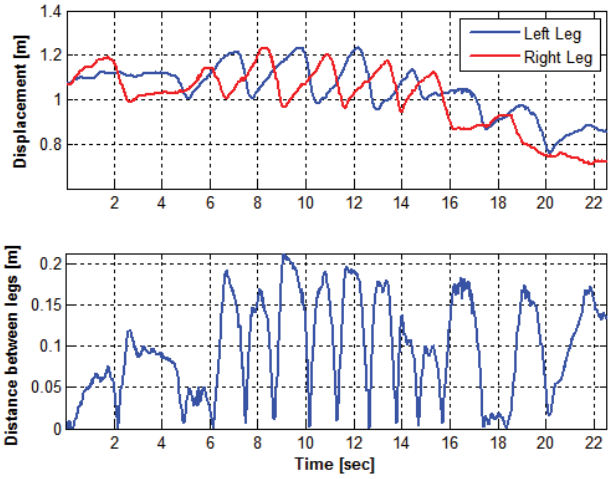

Fig. 7: Real experimental data from one subject's walking motion that have been used in the testing and evaluation phase of the constructed HMM. Top: Left (blue data) and Right (red data) legs displacement. Bottom: legs distance in the sagittal plane.

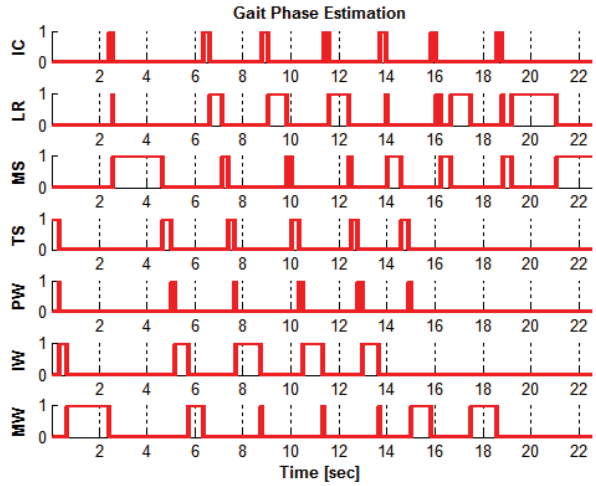

Fig. 8: Estimated sequence of gait phases based on the constructed model with respect to time by testing the data depicted in Fig. 7, which represent an unknown walking section.

to an underlying pathology.

There is an assumption, without loss of generality, that at the beginning of each gait cycle the initial contact refers to the left leg, while a complete stride is concluded when the right leg is again in front of the left leg, ready for a new initial contact and therefore for the next stride. By observing the results depicted in Fig. 8, it can be seen that the model manages to successfully recognize that (for the recorded experimental data of Fig. 7, used in this case study for model testing) the subject starts the motion with the right leg. Thus, the first estimated gait phase in Fig. 8 is the Terminal Stance (TS).

Another remark concerns the abnormal walking motion. At some point of the recorded test data of Fig. 7 (after 16*sec*), it can be seen that the motion is characterized by abnormal behaviour, and therefore the gait phase evaluation procedure has typical abnormal exports. Although the walking motion starts a new stride with the left leg, due to the abnormal nature of the data, the model could not recognize a complete stride. The results show that the constructed model recognizes the pathological gait.

D. Gait Parameters Computation Results

In order to perform the assessment of the impairment level of each patient, it is necessary to compute the appropriate gait parameters from which we can infer the pathological state. We have used the recognized sequence of gait phases and therefore the timestamps of each gait phase along with the estimated positions of the legs from the laser data to compute these parameters. The data are presented as the mean quantity plus/minus its standard deviation and refer to the patient's motion depicted and analysed in Fig. 7, 8. The presented gait patterns refer to a female patient, aged 77 years old with height 159cm, weight 60kg and knee height 45.5cm. Medical partners performed cognitive and mobility evaluation, in which this patient was categorised in cognitive level 1, i.e. no cognitive impairment and in mobility level 2, i.e. mild/moderate impairment - gait speed$< 0.6m/sec$ for unassisted walking.

The respective gait parameters for this patient are presented in Table I. The gait parameters will be useful for the formulation of a pathology recognition system based on the recognised gait patterns. We are currently working along with clinicians for the evaluation of those parameters and their categorization according to certain pathologies that result in mobility inabilities. The information about the patient's pathological state will then be used in the Context-Aware Robot Control for the assessment of the impairment level of the patient, and thus the inference of the patient's pathological status will trigger certain control assistive behaviors to be executed by the robotic assistant platform.

Parameters	
Right Step Length (m)	0.0565 ± 0.0147
Left Step Length (m)	0.1298 ± 0.0245
Stride Length (m)	0.1863 ± 0.0376
Step Width (m)	0.1688 ± 0.058
Cadence (step/min)	53.38
Stance time % of gait cycle	57.5
Swing time % of gait cycle	42.5

TABLE I: Gait Parameters computed using the range data and the segmentation in time of the recognised gait phases

VIII. Conclusions and Future Work

In this paper we have presented the basic concept of an Adaptive Context-Aware Robot Control architecture for a robotic assistant platform, that is moving in front of the the user, and will adapt to the user's needs in order to act assistively whenever in case. We have analysed the parts

of the proposed control scheme. Firstly, we have described the processing of the raw data from a laser range scanner mounted on the robotic platform. We have analysed the usage of a Kalman Filter for the tracking of the subject's legs and therefore the estimation of the legs' position and velocity, which are the input signal of the control scheme. Then, a Hidden Markov Model based framework have been represented in order to analyse the pathological walking motion, by detecting sequences of gait phases, constituting a completely non-invasive approach, since we have used a non-wearable device. The resulted sequence of the gait phases and the time segmentation are appropriate in order to compute specific gait parameters, necessary for clinical diagnosis.

For further research, we are working on a new detection and tracking system based on particle filtering, fusing also other sensorial data like RGB data, for a whole body tracking approach. Particle filters will perform better in more complicate motion scenarios including also turnings, that are not easy to track with Kalman Filter, which is a linear estimator. Moreover, particle filters can be better used for hierarchical tracking of the human body parts. Furthermore, we are working on the classification approach of normal/pathological gait or non-walking activity. Moreover, in assistance with clinicians, we are elaborating on the computed gait parameters from various patients, in order to organize and classify them according to certain pathologies. In that way, a complete automatic pathology recognition system will be developed in order to assess the impairment level of the patient, and particular levels of mobility impairment will indicate the need for specific control assistive actions for the robotic platform in order to adapt to the user's needs.

REFERENCES

[1] P. D. Foundation, "Statistics for parkinson's disease," 2010. [Online]. Available: http://www.pdf.org

[2] S. Center, "Stroke statistics," 2010. [Online]. Available: http://www.strokecenter.org

[3] M. Montemerlo, J. Pineau, N. Roy, S. Thrun, and V. Verma, "Experiences with a mobile robotic guide for the elderly," in *Proc. of National Conf. on AI*, 2002.

[4] X.Papageorgiou, C.Tzafestas, and et al, "Advances in intelligent mobility assistance robot integrating multimodal sensory processing," *Lecture Notes in Computer Science, Universal Access in Human-Computer Interaction. Aging and Assistive Environments*, vol. 8515, pp. 692–703, 2014.

[5] N. Hirai and H. Mizoguchi, "Visual tracking of human back and shoulder for person following robot," in *Advanced Intelligent Mechatronics, 2003. AIM 2003. Proceedings. 2003 IEEE/ASME International Conference on*, vol. 1, July 2003, pp. 527–532 vol.1.

[6] R. Luo, N.-W. Chang, S.-C. Lin, and S.-C. Wu, "Human tracking and following using sensor fusion approach for mobile assistive companion robot," in *Industrial Electronics, 2009. IECON '09. 35th Annual Conference of IEEE*, Nov 2009, pp. 2235–2240.

[7] S. Dubowsky, F. Genot, S. Godding, H. Kozono, A. Skwersky, H. Yu, and L. S. Yu, "Pamm - a robotic aid to the elderly for mobility assistance and monitoring: A 'helping-hand' for the elderly," in *IEEE Int'l Conf. on Robotics and Automation*, 2000, pp. 570–576.

[8] M. Spenko, H. Yu, and S. Dubowsky, "Robotic personal aids for mobility and monitoring for the elderly," *IEEE Trans. on Neural Systems and Rehabilitation Engineering*, vol. 14, no. 3, pp. 344–351, 2006.

[9] S. Jiang, B. Zhang, and D. Wei, "The elderly fall risk assessment and prediction based on gait analysis," in *IEEE 11th Int'l Conf. on Computer and Information Technology (CIT), 2011*, 2011, pp. 176–180.

[10] M. Bachlin, M. Plotnik, D. Roggen, I. Maidan, J. Hausdorff, N. Giladi, and G. Troster, "Wearable assistant for parkinson's disease patients with the freezing of gait symptom," *IEEE Trans. on Information Technology in Biomedicine*, vol. 14, no. 2, pp. 436–446, 2010.

[11] J. F.-S. Lin and D. Kulic, "Automatic human motion segmentation and identification using feature guided hmm for physical rehabilitation exercises," in *IEEE Int'l Conf. on Intelligent Robots and Systems*, 2011.

[12] J. Bae and M. Tomizuka, "Gait phase analysis based on a hidden markov model," *Mechatronics*, vol. 21, no. 6, pp. 961 – 970, 2011.

[13] C. Nickel, C. Busch, S. Rangarajan, and M. Mobius, "Using hidden markov models for accelerometer-based biometric gait recognition," in *Signal Processing and its Applications (CSPA), 2011 IEEE 7th Int'l Colloquium on*, 2011, pp. 58–63.

[14] I. Pappas, M. Popovic, T. Keller, V. Dietz, and M. Morari, "A reliable gait phase detection system," *IEEE Trans. on Neural Systems and Rehabilitation Engineering,*, vol. 9, no. 2, pp. 113–125, 2001.

[15] G. Bebis, M. Nicolescu, M. Nicolescu, A. Tavakkoli, C. King, and R. Kelley, "An architecture for understanding intent using a novel hidden markov formulation," *Int'l Journal of Humanoid Robotics*, vol. 05, no. 02, pp. 203–224, 2008.

[16] M. Meng, Q. She, Y. Gao, and Z. Luo, "Emg signals based gait phases recognition using hidden markov models," in *Information and Automation (ICIA), 2010 IEEE Int'l Conf. on*, 2010, pp. 852–856.

[17] A. Panangadan, M. Mataric, and G. Sukhatme, "Tracking and modeling of human activity using laser rangefinders," *Int'l Journal of Social Robotics*, vol. 2, no. 1, pp. 95–107, 2010. [Online]. Available: http://dx.doi.org/10.1007/s12369-009-0043-1

[18] X. Shao, H. Zhao, K. Nakamura, R. Shibasaki, R. Zhang, and Z. Liu, "Analyzing pedestrians' walking patterns using single-row laser range scanners," in *Systems, Man and Cybernetics, 2006. SMC '06. IEEE Int'l Conf. on*, vol. 2, 2006, pp. 1202–1207.

[19] K.Arras, S.Grzonka, M.Luber, and W.Burgard, "Efficient people tracking in laser range data using a multi-hypothesis leg-tracker with adaptive occlusion probabilities," in *Trans. of IEEE ICRA*. IEEE Int'l Conf. on Robotics and Automation, May 19-23.

[20] R. Kirby, J. Forlizzi, and R. Simmons , "Natural person-following behavior for social robots," in *Proceedings of Human-Robot Interaction*, March 2007, pp. 17–24.

[21] E.-J. Jung, B.-J. Yi, and S. Yuta, "Control algorithms for a mobile robot tracking a human in front," in *Intelligent Robots and Systems (IROS), 2012 IEEE/RSJ International Conference on*, Oct 2012, pp. 2411–2416.

[22] H. Zender, P. Jensfelt, and G. Kruijff, "Human- and situation-aware people following," in *Robot and Human interactive Communication, 2007. RO-MAN 2007. The 16th IEEE International Symposium on*, Aug 2007, pp. 1131–1136.

[23] A. Cosgun, D. Florencio, and H. Christensen, "Autonomous person following for telepresence robots," in *Robotics and Automation (ICRA), 2013 IEEE International Conference on*, May 2013, pp. 4335–4342.

[24] T. Kruse, A. K. Pandey, R. Alami, and A. Kirsch, "Human-aware robot navigation: A survey," *Robotics and Autonomous Systems*, vol. 61, no. 12, pp. 1726 – 1743, 2013.

[25] D. Ho, J.-S. Hu, and J.-J. Wang, "Behavior control of the mobile robot for accompanying in front of a human," in *Advanced Intelligent Mechatronics (AIM), 2012 IEEE/ASME International Conference on*, July 2012, pp. 377–382.

[26] X. S. Katsuyuki Nakamura, Huijing Zhao and R. Shibasaki, *Human Sensing in Crowd Using Laser Scanners, Laser Scanner Technology*, 2012.

[27] L. R. Rabiner, "Readings in speech recognition," A. Waibel and K.-F. Lee, Eds. San Francisco, CA, USA: Morgan Kaufmann Publishers Inc., 1990, ch. A tutorial on hidden Markov models and selected applications in speech recognition, pp. 267–296.

[28] A. Katsamanis, G. Papandreou, and P. Maragos, "Audiovisual-to-articulatory speech inversion using active appearance models for the face and hidden markov models for the dynamics." in *ICASSP*. IEEE, 2008, pp. 2237–2240.

[29] S. Theodorakis, A. Katsamanis, and P. Maragos, "Product-hmms for automatic sign language recognition." in *ICASSP*. IEEE, 2009, pp. 1601–1604.

[30] P. Turaga, R. Chellappa, V. S. Subrahmanian, and O. Udrea, "Machine recognition of human activities: A survey," *Circuits and Systems for Video Technology, IEEE Trans. on*, vol. 18, no. 11, pp. 1473–1488, 2008.

[31] C. Chen, J. Liang, H. Zhao, and H. Hu, "Gait recognition using hidden markov model," in *Advances in Natural Computation*, ser. Lecture Notes

in Computer Science, L. Jiao, L. Wang, X.-b. Gao, J. Liu, and F. Wu, Eds. Springer Berlin Heidelberg, 2006, vol. 4221, pp. 399–407.
[32] X. Papageorgiou, G. Chalvatzaki, C. Tzafestas, and P. Maragos, "Hidden markov modeling of human normal gait using laser range finder for a mobility assistance robot," in *Proc. of the 2014 IEEE Int'l Conf. on Robotics and Automation (ICRA)*, 2014.
[33] G. Chalvatzaki, G. Pavlakos, K. Maninis, X. Papageorgiou, V. Pitsikalis, C. Tzafestas, and P. Maragos, "Towards an intelligent robotic walker for assisted living using multimodal sensorial data," in *Mobihealth*, Nov 2014.
[34] O. Arias-Enriquez, M. Chacon-Murguia, and R. Sandoval-Rodriguez, "Kinematic analysis of gait cycle using a fuzzy system for medical diagnosis," in *NAFIPS 2012*, 2012.
[35] D. Arthur and S. Vassilvitskii, "K-means++: The advantages of careful seeding," in *Proc. of the 18th Annual ACM-SIAM Symposium on Discrete Algorithms*, ser. SODA '07, 2007.
[36] P. S. Maybeck, *Stochastic models, estimation and control*, ser. Mathematics in science and engineering. Academic Press NYC, 1979, vol. 1.
[37] M. Jacquelin Perry, *Gait Analysis: Normal and Pathological Function*, 1st ed., C. Bryan Malas, MHPE, Ed. SLACK Incorporated, 1992.
[38] A. Muro-de-la Herran, B. Garcia-Zapirain, and A. Mendez-Zorrilla, "Gait analysis methods: An overview of wearable and non-wearable systems, highlighting clinical applications," *Sensors*.
[39] S. Gamse, F. Nobakht-Ersi, and M. A. Sharifi, "Statistical process control of a kalman filter model," *Sensors*, vol. 14, no. 10, pp. 18 053–18 074, 2014. [Online]. Available: http://www.mdpi.com/1424-8220/14/10/18053
[40] J. Perry, *Gait Analysis: Normal and Pathological Function*. Slack Incorporated, 1992.